# An Adaptive Partition Strategy of Galerkin Boundary Element Method for Capacitance Extraction


Shengkun Wu
shengkunwu@foxmail.com
Peng Cheng Laboratory
Shenzhen, China

Biwei Xie
xiebiwei@ict.ac.cn
Institute of Computing Technology,
Chinese Academy of Sciences,
Beijing, China
Peng Cheng Laboratory
Shenzhen, China

Xingquan Li
fzulxq@gmail.com
School of Mathematics and Statistics,
Minnan Normal University
Zhangzhou, China
Peng Cheng Laboratory
Shenzhen, China



## ABSTRACT

In advanced process, electromagnetic coupling among interconnect wires plays an increasingly important role in signoff analysis. For VLSI chip design, the requirement of fast and accurate capacitance extraction is becoming more and more urgent. And the critical step of extracting capacitance among interconnect wires is solving electric field. However, due to the high computational complexity, solving electric field is extreme timing-consuming. The Galerkin boundary element method (GBEM) was used for capacitance extraction in [2]. In this paper, we are going to use some mathematical theorems to analysis its error. Furthermore, with the error estimation of the Galerkin method, we design a boundary partition strategy to fit the electric field attenuation. It is worth to mention that this boundary partition strategy can greatly reduce the number of boundary elements on the promise of ensuring that the error is small enough. As a consequence, the matrix order of the discretization equation will also decrease. We also provide our suggestion of the calculation of the matrix elements. Experimental analysis demonstrates that, our partition strategy obtains a good enough result with a small number of boundary elements.



## CCS CONCEPTS

• **Hardware → Electronic design automation**.

## KEYWORDS

Galerkin method, boundary element method, boundary partition, capacitance extraction

**ACM Reference Format:**
Shengkun Wu, Biwei Xie, and Xingquan Li. 2023. An Adaptive Partition Strategy of Galerkin Boundary Element Method for Capacitance Extraction. In *28th Asia South Pacific Design Automation Conference (ASPDAC '23), Janurary 16–19, 2023, Tokyo, Japan.* ACM, New York, NY, USA, 6 pages. https://doi.org/10.1145/3566097.3567903




*ASPDAC '23, Janurary 16–19, 2023, Tokyo, Japan*



ACM ISBN 978-1-4503-9783-4/23/01…$15.00
https://doi.org/10.1145/3566097.3567903


## 1 INTRODUCTION

With the feature size of integrated circuit scaling down, the coupling capacitance of interconnect wires is making more and more significant impact on circuit performance. The most of existed mature technologies of field solver are based on numerical approach. There are mainly several capacitance extraction methods which are the finite difference method (FDM), the finite element method (FEM), the boundary element method (BEM) and the floating random walk (FRW) method. These methods are called field solver.

The FEM and the FDM are classified as the domain discretization method. It usually produces a sparse matrix with large order, see [15] and [12]. In 3-D capacitance extraction, because the order of the matrix increase rapidly, the speed of this method is limited. However, the domain discretization method is well established, thus this method is also used by some software.

The FRW algorithm for capacitance extraction, presented as a 2-D version, was proposed in 1992 [4] . Its idea is to convert the calculation of conductor charge to the Monte Carlo integration performed with FRWs. The random walk method is advantageous in parallelism over the traditional methods, see [6] and [16]. Recently, the FRW method has been made a lot of progress. However, unlike the classical analytic method, the error of FRW is random.

The boundary element method [1] only needs to discretize the boundary, thus the matrix order produced by the BEM is smaller than that produced by the FDM. However, the matrix obtained by the BEM is not sparse and a lot of time is spent on calculating the matrix elements. There are several versions of the boundary element method, see [8] , [10] [13] and [2]. In [2], the authors used the Galerkin method and they used the multipole-accelerated boundary element method to caculate the matrix elements. In [3], a fast inverse of linear complexity was developed to solve a dense system of linear equations directly for the capacitance extraction.

In contrast to previous works, we focus on the matrix order reduction and study the boundary partition strategy. For this purpose, we use some mathematical theorems and physical approximation methods to provide a guidance of boundary partition strategy. Thus, the boundary partition strategy is rarely influenced subjectively. On the other hand, we will also propose our suggestion on the calculation of the matrix elements.

The Garlerkin method for the Laplace equation has been studied in Mathematics for a long time, see [9] and [5]. Its advantage is that it has an error estimation which can guide us to partition the boundary. With this guidance, we only need a small number of boundary elements to obtain high accuracy.

The main contributions of this paper are summarized as follows:

- For the electric charge calculation on single dielectric cases, we achieve a theoretical error estimation. The error estimation is obtained by several theorems of the Galerkin method and integral operators involved in the boundary integral equation.
- Honoring the guide of our error estimation, we develop a boundary partition scheme to adapt the electric field attenuation. Due to the fitness, this boundary partition strategy can largely reduce the number of boundary elements and ensure sufficient accuracy. Furthermore, the matrix order of the discretization equation will also greatly decrease.
- To calculate the matrix elements quickly, we present a hybrid analytical integration and numerical calculation approach.

The remainder of this paper is organized as follows. In Section 2, we provide the basic conception of the boundary element method. In Section 3, we analysis the error of Galerkin boundary element method and provide a boundary partition strategy. In Section 4, we discuss the multi-dielectric case. Section 5 shows experimental results.

## 2 PRELIMINARIES

In this section, we show that the capacitance extracting problem is equivalent to solve a boundary integral equation.

### 2.1 Problem Statement

In each dielectric region $\Omega_a$, see Figure 1, the electric potential $u_a$ satisfies the Laplace equation

$$\begin{cases} \nabla^2 u_a = 0 \text{ in } \Omega_a \\ u_a = 1 \text{ on the main conductor} \\ u_a = 0 \text{ on other conductors and the Dirichlet boundary} \\ \dfrac{\partial u_a}{\partial n} = 0 \text{ on the Neumann boundary.} \end{cases}$$

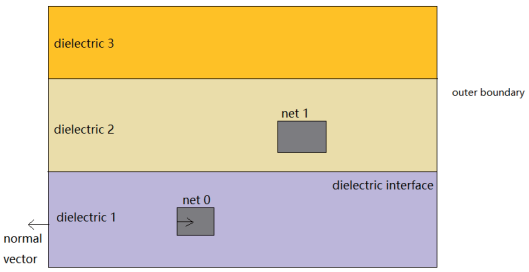


**Figure 1: A cross section of 3-D capacitance extraction problem with multi-dielectrics**

Let $q_a$ and $q_b$ be the normal electric field intensity on the boundaries of $\Omega_a$ and $\Omega_b$ respectively. On the dielectric interface $\Gamma_{ab}$ of two dielectric regions $\Omega_a$ and $\Omega_b$, the compatibility equation holds:

$$\varepsilon_a q_a = -\varepsilon_b q_b$$
$$u_a = u_b.$$

Using Green's identity [1], we have following equation:

$$\sigma(x)u_a(x) + \int_{\partial\Omega_a} q^*(x,y)u_a(y)dy = \int_{\partial\Omega_a} u^*(x,y)q_a(y)dy, \quad (1)$$

where

$$q^*(x,y) = \frac{\langle x-y, n_y\rangle}{4\pi|x-y|^3} \quad , \quad u^*(x,y) = \frac{1}{4\pi|x-y|}$$

and $\sigma(x)$ satisfies $\sigma(x) = \frac{1}{2}$ for almost all $x \in \partial\Omega_a$.

### 2.2 Classical Boundary Element Method

The classical boundary element method [11] employs boundary element partition and evaluating the boundary integral equation at collocation points, one for an element. The discretized boundary integral equation in the region $\Omega_a$ is

$$\sigma(x)u(x) + \sum_j u_j \int_{\Gamma_j} q^*(x,y)dy = \sum_j q_j \int_{\Gamma_j} u^*(x,y)dy.$$

### 2.3 Galerkin Method

Next, we discuss the single dielectric case with the Dirichlet boundary condition:

$$u = 0 \quad \text{on the outer boundary of the dielectric.}$$

Let $-\partial mcd$ represent the boundary of the main conductor ($mcd$) and the normal vectors point to the internal side of the main conductor. Then, the basic theory of electromagnetism tells us that

$$\int_{\partial\Omega} u^*(x,y)q(y)dy = f_0(x), \quad (2)$$

where

$$f_0(x) = \begin{cases} 1 & \text{if x is on } \partial mcd \\ 0 & \text{otherwise.} \end{cases}$$

To solve $q$, we need to partition the boundary to finite pieces. We suppose $\partial\Omega = \bigcup_j I_j$ and use $q_j$ to approximate $q(x)$ when $x \in I_j$, then we get following equation:

$$\sum_j \left( \int_{I_j} u^*(x,y)dy \right) q_j = f_0(x).$$

Integrating both sides over $I_i$, we get

$$\sum_j \left( \int_{I_i}\int_{I_j} u^*(x,y)dydx \right) q_j = \int_{I_i} f_0(x)dx. \quad (3)$$

This is the Garlerkin method discussed in [2]. Once we have solved this equation, the electric charge on the boundary $\partial cd_k$ of the $k$-th conductor ($cd_k$) is given by

$$Q_k' = \sum_{I_j \subset \partial cd_k} \varepsilon q_j |I_j|, \quad (4)$$

where $\varepsilon$ is the dielectric constant. Let

$$A = \left\{ \frac{1}{|I_i|}\frac{1}{|I_j|} \int_{I_i}\int_{I_j} u^*(x,y)dydx \right\}_{i,j}. \quad (5)$$

To solve the equation, we need to know more about the information of the matrix $A$. It is easy to see that $A$ is symmetric. In fact, we can show that $A$ is positive definite. Moreover, we will give an error estimation of the electric charge on each conductor, through this estimation we will state our strategy of how to partition the boundary.

# 3 SINGLE DIELECTRIC CASE

## 3.1 Error Estimation of Capacitance

To achieve our goals, we need two theorems. Let $V$ be an operator such that

$$Vq(x) = \int_{\partial\Omega} u^*(x,y)q(y)dy.$$

**Theorem** 1. *[9, Theorem 6.22] If the dimension of the region is three, then the operator $V$ is elliptic on the Sobolev space $H^{-1/2}(\partial\Omega)$ , i.e.*

$$\langle Vg, g\rangle \geq c\|g\|^2_{H^{-1/2}(\partial\Omega)} \text{ for all } g \text{ in } H^{-1/2}(\partial\Omega).$$

By Theorem 1, we know that the operator $V$ is positive definite and bounded below. In fact, this kind of operators is called elliptic operators. As a consequence, the matrix $A$ defined via (5) is positive definite. Once the matrix is symmetric and positive definite, the Cholesky decomposition is an efficient way to solve (3).

**Theorem** 2. *[9, Lemma 8.1] If $V$ is a bounded operator from Banach space $X$ to its dual space $X^{'}$ and elliptic operator on $X$. Let $q$ be a solution of the equation*

$$Vq = f \text{ given } f \in X^{'}.$$

*Let $X_m$ be a finite dimensional subspace of $X$, and $q^{'} \in X_m$ be the solution of following equation*

$$\langle Vq', p\rangle = \langle f, p\rangle \text{ for all } p \in X_m. \tag{6}$$

*We have*

$$\|q - q'\|_X \leq C \inf_{p\in X_m} \|q - p\|_X.$$

Equation (6) is called Galerkin Scheme. To apply Theorem 2, let $X_m$ the linear span of functions $\left\{\frac{\chi_{I_j}}{|I_j|}\right\}$, where

$$\chi_{I_j}(x) = \begin{cases} 1 & \text{if x is on } I_j \\ 0 & \text{otherwise.} \end{cases}$$

Thus $X_m$ is a finite dimensional subspace of $H^{-1/2}(\partial\Omega)$. Then (2) is equivalent to

$$\langle Vq', \frac{\chi_{I_i}}{|I_i|}\rangle = \langle f, \frac{\chi_{I_i}}{|I_i|}\rangle.$$

Since $q^{'} \in X_m$, we suppose $q^{'} = \sum_j c_j\chi_{I_j}$. Thus

$$\sum_j \left(\frac{1}{|I_i|}\frac{1}{|I_j|}\int_{I_i}\int_{I_j} u^*(x,y)dydx\right) c_j|I_j| = \langle f, \frac{\chi_{I_i}}{|I_i|}\rangle.$$

Comparing this equation with (3), we know that equation (3) coincides with the Galerkin method (6) and the relationship is given by

$$q^{'} = \sum_j q_j\chi_{I_j},$$

where $q^{'}$ is the solution of the Galerkin method (6) and $\{q_j\}$ comes from (3). We will use this relationship to provide an error estimation of our method.

**Proposition** 1. *Let $Q_k$ be the electric charge on the conductor $k$. Let $Q_k^{'}$ be the electric charge on the conductor $k$ obtained by (4). The projection of $q \in H^{-1/2}(\partial\Omega)$ onto $X_m$ is given by*

$$P_m q = \sum_j \frac{1}{|I_j|}\int_{I_j} q(x)dx\chi_{I_j},$$

*then there is a constant such that*

$$|Q_k - Q_k^{'}| \leq C\|q - P_m q\|_{L^2(\partial\Omega)}.$$

*If the tangential derivative of $q$ on the boundary exists, we further have*

$$|Q_k - Q_k^{'}| \leq C \sup_j \left(|I_j| \sup_{x\in I_j} \frac{\partial q}{\partial\tau}(x)\right).$$

**Proof:** Based on Gauss's Theorem, we have

$$\begin{aligned}
|Q_k - Q_k^{'}| &= \left|\varepsilon\int_{\partial cd_k} q(x)d\Gamma(x) - \sum_{I_j\subset\partial cd_k} \varepsilon q_j|I_j|\right| \\
&= \varepsilon\left|\int_{\partial cd_k} q(x) - q^{'}(x)dx\right| \\
&= \varepsilon\left|\langle(q(x) - q^{'}(x)), \chi_{\partial cd_k}\rangle\right| \\
&\leq \varepsilon\|q(x) - q^{'}(x)\|_{H^{-1/2}(\partial\Omega)}\|\chi_{\partial cd_k}\|_{H^{1/2}(\partial\Omega)} \\
&= \varepsilon|\partial cd_k|\cdot\|q - q^{'}\|_{H^{-1/2}(\partial\Omega)}.
\end{aligned}$$

Using Theorem 2, we obtain

$$\|q - q^{'}\|_{H^{-1/2}(\partial\Omega)} \leq C \inf_{p\in X_m} \|q - p\|_{H^{-1/2}(\partial\Omega)}.$$

Thus

$$\begin{aligned}
|Q_k - Q_k^{'}| &\leq C\varepsilon|\partial cd_k| \inf_{p\in X_m} \|q - p\|_{H^{-1/2}(\partial\Omega)} \\
&\leq C\varepsilon|\partial cd_k| \inf_{p\in X_m} \|q - p\|_{L^2(\partial\Omega)} \\
&= C\varepsilon|\partial cd_k|\|q - P_m q\|_{L^2(\partial\Omega)}.
\end{aligned}$$

Further, if the tangential derivative of $q$ exists, then

$$\begin{aligned}
&|Q_k - Q_k^{'}| \\
\leq& C\varepsilon|\partial cd_k|\Big(\int_{\partial\Omega}\Big|q(x) - \sum_j \frac{1}{|I_j|}\int_{I_j} q(y)dy\chi_{I_j}(x)\Big|^2 dx\Big)^{1/2} \\
=& C_2\Big(\int_{\partial\Omega}\Big|\sum_j \frac{1}{|I_j|}\int_{I_j} q(x) - q(y)dy\chi_{I_j}(x)\Big|^2 dx\Big)^{1/2} \\
=& C_2\Big(\int_{\partial\Omega}\Big|\sum_j \frac{1}{|I_j|}\int_{I_j} |I_j| \sup_{x\in I_j}|\frac{\partial q}{\partial\tau}(x)|dy\chi_{I_j}(x)\Big|^2 dx\Big)^{1/2} \\
\leq& C_2|\partial\Omega|^{1/2} \sup_j \left(|I_j| \sup_{x\in I_j}|\frac{\partial q}{\partial\tau}(x)|\right)^{1/2}
\end{aligned}$$

to complete the proof. □

Proposition 1 gives the error of the electric charge on each conductor. Since the capacitance of the main conductor is given by $C_1 = Q_1$ and the coupling capacitance between the main conductor and the conductor $k$ is given by $C_k = -Q_k$, we can obtain the error estimation of each capacitance.

Proposition 1 tells us that the error is dominated by the area of the boundary element times the derivative of the electric field

intensity on that element. On the other hand, the boundary conditions tell us that the main conductor has electric potential 1 and other boundaries have electric potential 0, thus the derivative of the electric field intensity decreases rapidly as the distance to the main conductor increases. Thus, for the boundary element which is far away from the main conductor, the area of the boundary element can be very large due to the derivative of the electric potential is small. That is the reason that this method can reduce the number of boundary elements. Next, we provide several formulas for the boundary partition strategy.

### 3.2 Compact Boundary Partition

We suppose all conductors are constructed by cuboid. If a conductor is a trapezoid, we use several cuboids to approximate it.

Our boundary element partition strategy is based on Proposition 1. If we want to make the error small, we need to partition $\partial\Omega$ such that

$$|I_j| \sup_{x\in I_j} |\frac{\partial q}{\partial \tau}(x)| \le c$$

for some constant $c$ which is small. That is to say we want

$$|I_j| \le \frac{c}{\sup_{x\in I_j} |\frac{\partial q}{\partial \tau}(x)|}.$$

Because the region is irregular, it's very hard to obtain a priori estimate of $|\frac{\partial q}{\partial \tau}(x)|$. However, we can take a physical approximation from the boundary conditions of the capacitance extraction problem.

According to the boundary conditions, the electric field intensity decreases as the distance to the main conductor increases. We suppose that if the boundary is far away from the main conductor, then $|\frac{\partial q}{\partial \tau}(x)|$ is small. As a consequence the area of the responding boundary element can be large. If $x$ is far away from the main conductor, then we can regard the main conductor as a ball with radio $r$ and center $x_0$. If the electric potential of the ball is 1, then the electric field intensity of point $x$ is given by $q(x) = \frac{r^2}{|x-x_0|^2} \cdot \frac{x-x_0}{|x-x_0|}$. Thus we have

$$|\frac{\partial q}{\partial \tau}(x)| \le \frac{C}{|x-x_0|^3} \text{ for some constant } C. \tag{7}$$

Our partition strategy for the boundary which is far away from the main conductor is based on equation (7).

Now, we propose our strategy of partition. Let $p_1, p_2, p_3$ are parameters which can be chosen for different cases.

If the distance between the boundary and the main conductor is less than $p_1$, then we partition it to rectangles $\{I_j\}$ such that

$$|I_j| \le p_2.$$

If the distance of the boundary is larger than $p_1$, then we partition it to rectangles $\{I_j\}$ such that

$$|I_j| \le p_3 * p_2 * (d_{I_j}/p_1)^3,$$

where $d_{I_j}$ is the distance between $I_j$ and the main conductor. Due to the electric field shielding effect, if the outer normal vector of the boundary points to the main conductor, we set $p_3 = 1$ else we set $p_3$ to be larger than 1.

### 3.3 Fast Calculation of Matrix Elements

Because most of the run time of any kind of boundary element methods is spent computing matrix elements. It is crucial to compute matrix elements as fast as we can. The matrix elements are given by

$$a_{i,j} = \frac{1}{|I_i|}\frac{1}{|I_j|}\int_{I_i}\int_{I_j} u^*(x,y)dydx = \frac{1}{4\pi|I_i||I_j|}\int_{I_i}\int_{I_j}\frac{1}{|x-y|}dydx.$$

A fast algorithm of the calculation of $a_{i,j}$ is given by [7]. Several closed forms have been given, thus the computational complexity is small. Thus, we adopt the method in [7] to calculate matrix elements.

## 4 MULTI-DIELECTRIC CASE

### 4.1 Galerkin Method

In this section, we discuss the multi-dielectric case. Due to equation (1), we have

$$\sigma(x)u_a(x) + \int_{\partial\Omega_a} q^*(x,y)u_a(y)dy = \int_{\partial\Omega_a} u^*(x,y)q_a(y)dy,$$

holds for $x \in \Omega_a$. We partition the boundary such that $\partial\Omega = \bigcup_j I_j$. Taking integral over $I_i$ on both side and approximating $q_a(y)$ and $u_a(y)$ on each element with constant, we then obtain

$$\frac{1}{2}\int_{I_i} u_a dx + \sum_k \left(\int_{I_i}\int_{I_k} q^*(x,y)dydx\right) u_{a,k}$$
$$= \sum_j \left(\int_{I_i}\int_{I_j} u^*(x,y)dydx\right) q_{a,j}.$$

We obtained a linear equation. In the multi-dielectric case, we don't have an error estimation. However, we still use the partition strategy in Section 3.2 for boundaries of conductors and the outer boundary. But, we need to change the partition strategy for the boundary elements on the dielectric interface. Since the unknowns corresponding to these boundary elements include electric field intensity and electric potential.

If $x$ is far away from the main conductor, we suppose the electric potential satisfies

$$\left|\frac{\partial u}{\partial \tau}(x)\right| \le \frac{C}{|x-x_0|^2}.$$

Thus, for the dielectric interface, our partition strategy is as follows. If the distance between the boundary and the main conductor is less that $p_1$, then we partition it to rectangles $\{I_j\}$ such that

$$|I_j| \le p_2.$$

If the distance of the boundary is larger that $p_1$, then we partition it to rectangles $\{I_j\}$ such that

$$|I_j| \le p_2 * p_3 * (d_{I_j}/p_1)^2,$$

where $d_{I_j}$ is the distance between $I_j$ and the main conductor.

### 4.2 Fast Calculation of Matrix Elements

The matrix elements include two kind of integrals:

$$A_{i,j} = \int_{I_i}\int_{I_j} u^*(x,y)dydx \quad \text{and} \quad Q_{i,j} = \int_{I_i}\int_{I_j} q^*(x,y)dydx.$$

The first one have been discussed in Section 3.3.

To handle the integral, we need some notations. If $f(x)$ is a function, we denote

$$D_x(x_u, x_d)f(x) = f(x_u) - f(x_d)$$

and

$$\begin{aligned} &D_{x_1,\cdots,x_n}(x_{1u}, x_{1d}, \cdots, x_{nu}, x_{nd}) \\ =&D_{x_1}(x_{1u}, x_{1d})D_{x_2,\cdots,x_n}(x_{2u}, x_{2d}, \cdots, x_{nu}, x_{nd}). \end{aligned}$$

Let $\vec{n}(I_i)$ and $\vec{n}(I_j)$ be the normal vector of $I_i$ and $I_j$ respectively. We are going to consider several situations by discussing the directions of $\vec{n}(I_i)$ and $\vec{n}(I_j)$.

If $\vec{n}(I_i)$ is parallel to $\vec{n}(I_j)$, we suppose $I_i$ and $I_j$ satisfies

$$\begin{aligned} I_i &= \{(x_1, x_2, x_3) : x_{1d} \le x_1 \le x_{1u}, x_{2d} \le x_2 \le x_{2u}\} \\ I_j &= \{(y_1, y_2, y_3) : y_{1d} \le y_1 \le y_{1u}, y_{2d} \le y_2 \le y_{2u}\}. \end{aligned}$$

If $b = x3 - y3 = 0$, then by the formular of $q^*(x, y)$ we have $Q_{i,j} = 0$.

If $b = x3 - y3 \neq 0$, we have

$$\begin{aligned} Q_{i,j} =& \int_{x_{1d}}^{x_{1u}} \int_{x_{2d}}^{x_{2u}} \int_{y_{1d}}^{y_{1u}} \int_{y_{2d}}^{y_{2u}} \frac{\langle x - y, n_y \rangle}{4\pi|x - y|^3} dy_2 dy_1 dx_2 dx_1 \\ =&D_{x_1,y_1}(x_{1u}, x_{1d}, -y_{1u}, -y_{2d}) \int_{x_{2d}}^{x_{2u}} \int_{-y_{2d}}^{-y_{2u}} \\ &\frac{1}{4\pi} \frac{b\sqrt{(x_2 + y_2)^2 + (x_1 + y_1)^2 + b^2}}{(x_2 + y_2)^2 + b^2} dx_2 dy_2. \end{aligned}$$

For any function $G$, we have

$$\begin{aligned} &\int_{x_d}^{x_u} \int_{y_d}^{y_u} G(x + y) dy dx \Big(\text{Let } \delta x = x_u - x_d, \delta y = y_u - y_d.\Big) \\ =& \int_0^{\delta y} uG(u + x_d + y_d) du + \int_{\delta x}^{\delta y} \delta y G(u + x_d + y_d) du \\ &+ \int_{\delta x}^{\delta y + \delta x} (\delta y + \delta x - u) G(u + x_d + y_d) du. \end{aligned} \tag{8}$$

using (8), we can calculate $Q_{i,j}$.

If $\vec{n}(I_i)$ is orthogonal to $\vec{n}(I_j)$, we suppose $I_i$ and $I_j$ satisfies

$$\begin{aligned} I_i &= \{(x_1, x_2, x_3) : x_{1d} \le x_1 \le x_{1u}, x_{3d} \le x_3 \le x_{3u}\} \\ I_j &= \{(y_1, y_2, y_3) : y_{1d} \le y_1 \le y_{1u}, y_{2d} \le y_2 \le y_{2u}\}. \end{aligned}$$

Then

$$\begin{aligned} Q_{i,j} =& D_{x_3,x_1,y_1}(\tilde{x}_{3u}, \tilde{x}_{3d}, x_{1u}, x_{1d}, -y_{1u}, -y_{1d}) \\ &\int_{\tilde{y}_{2d}}^{\tilde{y}_{2u}} (x_1 + y_1) \ln \left[(x_1 + y_1) + \sqrt{(x_1 + y_1)^2 + y_2^2 + x_3^2}\right] \\ &- \sqrt{(x_1 + y_1)^2 + y_2^2 + x_3^2} dy_2. \end{aligned}$$

Thus, we can calculate $Q_{i,j}$ by using numerical integrals.

## 5 EXPERIMENTAL RESULTS

We implemented our Galerkin projection boundary element method (GBEM) in C++ programming language, and performed all the experiments on Linux workstation with Intel(R) Xeon(R) Gold 5218 server with CPU at 2.3 GHz. We validate the efficiency and effectiveness of our GBEM by designing several experiments on single dielectric and multiple dielectric, respectively.

There are several hyper-parameters $p_1, p_2, p_3$ as discussed in Subsection 3.2 and 4.1. For example, if the length of the main conductor is $l(\mu m)$, then we usually set $p_1$ to be $l(\mu m)$ and $p_2$ to be $0.2 * l(\mu m)$. $p_3$ is usually set to be 1 when the normal vector of the boundary is pointing to the main conductor 2 otherwise. $p_1, p_2, p_3$ can be adjusted in different situations.

### 5.1 Single Dielectric

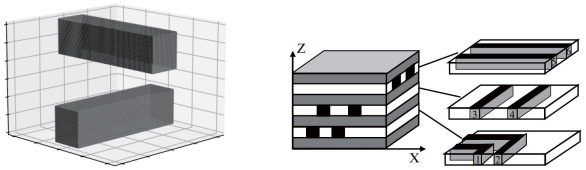


(a) Single-dielectric test case (b) multi-dielectric test case

**Figure 2: Test cases**

We first present the experimental result of a single dielectric case. We use the test case in [11, Page 55], as shown in Figure 2 (a). We suppose the electric potential is 0 on the dielectric boundary.

The comparison results of above cases obtained by our method GBEM with different numbers of boundary elements and [11, Page 55] are presented in Table 1. In the table, "GBEM(74)" means that GBEM with 74 boundary elements and "$C_{ii}$" is the capacitance of the conductor $i$ when the conductor $i$ is the main conductor. "Error1" and "Error2" are the error ratio with tool Raphael since we regard the commercial software Raphael as the golden. "Time(s)" gives the total runtime in second, and "Mem(MB)" gives the maximum resident memory required in MB (the same below). From Table 1, compared with the state-of-the-art works, our GBEM with 74 boundary elements can obtain the results with errors of less than 5% but achieve 46–406× speedup.

**Table 1: Capacitance calculated with different methods (in unit of $10^{-18}$ F).**

| Method | $C_{11}$ | Error1(%) | $C_{22}$ | Error2(%) | Time(s) | Mem(MB) |
|---|---|---|---|---|---|---|
| Raphael | 232.2 | 0 | 181.5 | 0 | – | – |
| GIMEI | 230 | 0.94 | 180.6 | 0.5 | 2.8 | 3.5 |
| FastCap | 226 | 2.7 | 176 | 3 | 24.37 | 22 |
| QMM | 221 | 4.86 | 176.4 | 2.81 | 4.98 | 5.1 |
| GBEM(74) | 222 | 4.4 | 178 | 1.93 | 0.06 | 7.19 |

### 5.2 Multiple Dielectric with BEM

Our multi-dielectric test case with six conductors comes from [11, Page 56], shown in Figure 2 (b). In this case the top and the bottom dielectric boundaries are Dirichlet boundaries. Other dielectric boundaries are Neumann boundaries. Other data of this case can be found in [11, Page 56]. In Table 2, we provide the capacitance obtain by [11] using different methods carried out on a Sun Ultra Enterprise 450 server. In Table 4, we present the details of our results, where "Panels" and "Cap." are the number of boundary elements and the capacitance.

**Table 2: The digonal entries of the capacitance matrices calculated with different methods (in unit of $10^{-15}$ F).**

| Method | $C_{11}$ | $C_{22}$ | $C_{33}$ | $C_{44}$ | $C_{55}$ | $C_{66}$ | Time(s) | Mem(MB) |
|---|---|---|---|---|---|---|---|---|
| ODDM | 0.68 | 1.29 | 1.57 | 1.52 | 2.54 | 2.54 | 122 | 2.7 |
| QMM | 0.682 | 1.31 | 1.6 | 1.54 | 2.53 | 2.53 | 58.4 | 3.80 |
| GBEM | 0.691 | 1.306 | 1.598 | 1.542 | 2.544 | 2.539 | 2.2 | 8.47 |

**Table 3: Comparison of RWCap(R) and GBEM (in unit of $10^{-16}$ F).**

| | RWCap(R) | | | | GBEM | | | | | | |
|---|---|---|---|---|---|---|---|---|---|---|---|
| Case | $C_{self}$ | $C_{cl}$ | Time(s) | Walks | $C_{self}$ | Dis. (%) | $C_{cl}$ | Dis.(%) | Time(s) | Speedup | Panels |
| 1 | 18.4 | 6.41 | 4.82 | 61k | 18.7 | 1.6 | 6.28 | 2.03 | 3.48 | 1.39 | 1920 |
| 2 | 19.51 | 5.47 | 1.52 | 56k | 19.5 | 0.05 | 5.5 | 0.55 | 2.61 | 0.58 | 1624 |
| 3 | 7.28 | 2.69 | 2.10 | 46k | 7.13 | 2.06 | 2.65 | 1.49 | 1.77 | 1.19 | 1624 |
| 4 | 3.65 | 1.67 | 4.93 | 51k | 3.62 | 0.82 | 1.63 | 2.4 | 0.538 | 9.16 | 1066 |
| 5 | 3.95 | 1.36 | 1.47 | 44k | 3.92 | 0.76 | 1.40 | 2.94 | 1.89 | 0.78 | 1922 |
| 6 | 1.44 | 0.517 | 3.31 | 51k | 1.46 | 1.39 | 0.494 | 4.45 | 0.674 | 4.91 | 1270 |

For the QMM method in [11], the number of boundary elements of a conductor ranges from 2277 to 2575 for capacitance computation. However, from Table 4, we can see that the number of boundary elements of a conductor in our GBEM only ranges from 217 to 316. In short, we save at least 87.13% boundary elements, which can greatly reduce the dimension of matrix in linear system of equations. Furthermore, this reduction on matrix dimension greatly contributes to speed up the runtime of capacitance computation.

**Table 4: Panels, times and memory for computing each capacitance (in unit of $10^{-15}$ F).**

| – | $C_{11}$ | $C_{22}$ | $C_{33}$ | $C_{44}$ | $C_{55}$ | $C_{66}$ | Avg. |
|---|---|---|---|---|---|---|---|
| Panels | 217 | 316 | 312 | 314 | 297 | 306 | 293 |
| Time(s) | 0.251 | 0.422 | 0.394 | 0.402 | 0.375 | 0.371 | 0.37 |
| Mem(MB) | 8.13 | 8.375 | 8.38 | 8.47 | 8.17 | 8.16 | 8.28 |
| Cap. | 0.691 | 1.306 | 1.598 | 1.542 | 2.544 | 2.539 | |

## 5.3 Multiple Dielectric with FRW

Recently, there are a lot of progress on the floating random walk (FRW) solver for capacitance. One of efficient and effectiveness algorithms is RWCap(R) in [14]. We provide a comparison of RWCap(R) and GBEM in Table 3. In Table 3, "$C_{self}$" is the capacitance of the main conductor, "$C_{cl}$" is the maximal coupling capacitance, "Dis." is the discrepancy ratio of our result against the result of RWCap(R), and "Speedup" is the ratio of our GBEM runtime to RWCap(R). The experiments in [14] are carried out on a Linux server with Intel Xeon E5620 8-core CPU of 2.40 GHz. Our test cases are the typical 180-nm and 45-nm technology available from [14]. The experimental results in Table 3 show that our GBEM speed up runtime about 3.00× than RWCap(R).

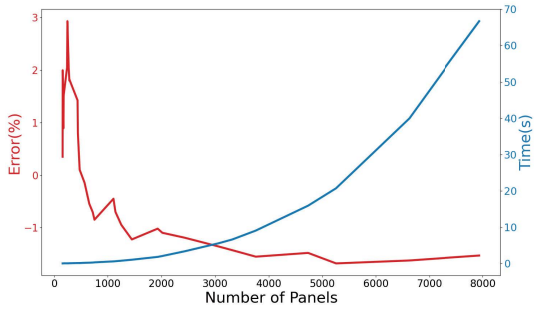


**Figure 3: The run time and error curve.**

To analyse the convergence tendency of our approach, we compute the capacitance of the conductor 1 in our multi-dielectric test case in Figure 2 (b) by partitioning the boundary to different numbers of panels. We got 31 groups of data and the numbers of the boundary elements ranges from 158 to 7935. We calculate the discrepancy from each capacitance to the mean and plot the runtime and error curve, see Figure 3. As we can see from the curve, we found that as the number of panels increases, the capacitance value converges to a limit.

## 6 CONCLUDING REMARKS

We proposed an error analysis of the Garlerkin boundary element method for the capacitance extraction. Based on the error analysis of this method, we proposed a boundary element partition strategy which can largely reduce the number of boundary elements. To calculate the matrix elements quickly, we proposed our method to deal with these integrals.

## ACKNOWLEDGMENTS

This work is supported in part by the Major Key Project of PCL (PCL2021A08), the National Natural Science Foundation of China (NSFC) (Grants No. 61907024), the Natural Science Foundation of Fujian Province (Grants No. 2020J05161).

## REFERENCES

[1] C. A. Brebbia. 1978. *The Boundary Element Method for Engineers.* Pentech Press, London.
[2] X. Cai, K. Nabors, and J. White. 1995. Efficient Galerkin techniques for multipole-accelerated capacitance extraction of 3-D structures with multiple dielectrics. In *Proceedings of the Conference on Advanced Research in VLSI.* 200–211.
[3] W. Chai, D. Jiao, and C.-K. Koh. 2009. A direct integral-equation solver of linear complexity for large-scale 3-D capacitance and impedance extraction. In *Proceedings of Design Automation Conference.* 752–757.
[4] L. L. Coz and R. B. Iverson. 1992. A stochastic algorithm for high speed capacitance extraction in integrated circuits. *Solid-State Electron* 35, 7 (1992), 1005–1012.
[5] J. Gwinner and E. P. Stephan. 2018. *Advanced Boundary Element Methods: Treatment of Boundary Value, Transmission and Contact Problems.* Springer, New York.
[6] G. Hu, W. Yu, H. Zhuang, and S. Zeng. 2011. Efficient floating random walk algorithm for interconnect capacitance extraction considering multiple dielectrics. In *Proceedings of IEEE International Conference on ASIC.* 896–899.
[7] Jitesh Jain, Cheng-Kok Koh, and Venkataramanan Balakrishnan. 2006. Exact and Numerically Stable Closed-Form Expressions for Potential Coefficients of Rectangular Conductors. *IEEE TRANSACTIONS ON CIRCUITS AND SYSTEMS—II: EXPRESS BRIEFS* 53, 6 (JUNE 2006), 200–211.
[8] W. Shi, J. Liu, N. Kakani, and T. Yu. 1998. Fast hierarchical algorithm for 3-D capacitance extraction. In *Proceedings of Design Automation Conference.* 212–217.
[9] Olaf Steinbach. 2008. *Numerical Approximation Methods for Elliptic Boundary Value Problems.* Springer, New York.
[10] W. Sun, W. Dai, and W. Hong. 1997. Fast parameter extraction of general interconnects using geometry independent measured equation of invariance. *IEEE Transactions on Microwave Theory and Techniques* 45 (1997), 827–836.
[11] W. Yu and X. Wang. 2014. *Advanced Field-Solver Techniques for RC Extraction.* Springer, New York.
[12] W. Yu and Z. Wang. 2005. Capacitance extraction. *Encyclopedia of RF and Microwave Engineering* (2005).
[13] W. Yu, Z. Wang, and J. Gu. 2003. Fast capacitance extraction of actual 3-D VLSI interconnects using quasi-multiple medium accelerated BEM. *IEEE Transactions on Microwave Theory and Techniques* 51 (2003), 109–119.
[14] W. Yu, H. Zhuang, C. Zhang, G. Hu, and Z. Liu. 2013. RWCap: A floating random walk solver for 3-D capacitance extraction of very-large-scale integration interconnects. *IEEE Transactions on Computer-Aided Design of Integrated Circuits and Systems* 32, 3 (2013), 353–366.
[15] A. H. Zemanian. 1988. A finite-difference procedure for the exterior problem inherent in capacitance computation for VLSI interconnects. *IEEE Transactions on Electron Devices* 35, 12 (July 1988), 985–992.
[16] C. Zhang and W. Yu. 2014. Efficient techniques for the capacitance extraction of chip-scale VLSI interconnects using floating random walk algorithm. In *Proceedings of Asia South Pacific Design Automation Conference.* 756–761.